

Generation and Evolution of Internal Waves in Luzon Strait

Ren-Chieh Lien
Applied Physics Laboratory
University of Washington
1013 NE 40th Street
Seattle, Washington 98105
Phone: (206) 685-1079 fax: (206) 543-6785 email: lien@apl.washington.edu

Frank Henyey
Applied Physics Laboratory
University of Washington
1013 NE 40th Street
Seattle, Washington 98105
Phone: (206) 543-4865 fax: (206) 543-6785 email: frank@apl.washington.edu

Award Number: N00014-09-1-0279

LONG-TERM GOALS

Our long-term scientific goals are to understand the dynamics and identify mechanisms of small-scale processes—i.e., internal tides, inertial waves, nonlinear internal waves (NLIWs), and turbulence mixing—in the ocean and thereby help develop improved parameterizations of mixing for ocean models. Mixing within the stratified ocean is a particular focus as the complex interplay of internal waves from a variety of sources and turbulence makes this a current locus of uncertainty. For this study, our focus is on the generation, propagation, evolution, and dissipation of small-scale internal waves and internal tides as the Kuroshio and barotropic tides interact with the two prominent submarine ridges in Luzon Strait.

OBJECTIVES

The primary objectives of this observational program are to quantify 1) the generation of NLIWs and internal tides in the vicinity of Luzon Strait, 2) the energy flux of NLIWs and internal tides into the Pacific Ocean and South China Sea (SCS), 3) the effects of the Kuroshio on the generation and propagation of NLIWs and internal tides, 4) the seasonal variation of NLIWs and internal tides, and 5) to study other small-scale processes, e.g., hydraulics and instabilities along internal tidal beams and at the Kuroshio front.

APPROACH

Near-field

In the Luzon Strait (Fig. 1), observations were taken using the combined 600-m-long towed CTD chain (TOWCTD) equipped with 40 CTD sensors and the Doppler sonar on the R/V *Revelle*. These

instruments took high-frequency, $\Delta t < 1$ min, and high vertical resolution, $\Delta z = 5\text{--}20$ m, measurements of temperature, salinity, and density, and oceanic velocity from near the surface to ~ 600 -m depth.

Far-field

Full water column velocity and temperature observations were taken using one subsurface mooring with a near-bottom upward-looking 75-kHz ADCP and one surface mooring with three ADCPs, temperature loggers, and a series of CTD sensors at a sampling rate of $\Delta t = 1$ min, capable of measuring internal tides and NLIWs on the continental slope east of Dongsha Island, ~ 200 n mi west of Luzon Strait (Fig. 1).

WORK COMPLETED

Near-field Experiment

From 25 July through 4 August 2011, we conducted an intensive survey in the Luzon Strait using a 600-m-long towed system (TOWCTD) equipped with 20–40 CTD sensors. The TOWCTD was developed specifically for this experiment. It provides CTD observations via inductive modem allowing us to identify the energetic small-scale processes in real time. All CTD sensors sample temperature, salinity, and pressure at a 10-s interval. The primary scientific objectives of this cruise were 1) to measure nonlinear internal waves in Babuyan channel, 2) to measure lee waves behind the sill west of Babuyan channel, 3) to quantify internal tide generation in southern Luzon Strait, and 4) to measure internal tide evolution in southern Luzon Strait.

Far-field Experiment

One surface buoy mooring (TC1), one subsurface mooring (TC2), and two bottom pressure moorings (TC1-BPR and TC2-BPR) were deployed on the Dongsha slope from the Taiwanese R/V *Ocean Researcher 1* on 27–31 May 2011. The surface and subsurface moorings were placed 6 km apart on the slope. Three ADCPs, fourteen CTD sensors, and three temperature loggers were equipped on the surface mooring (TC1). The subsurface mooring (TC2) was equipped with one 75-kHz ADCP, ten temperature sensors, and three CTD sensors. On 1–6 June 2011 the surface and subsurface moorings were recovered by the Taiwanese R/V *Ocean Researcher 2*. The subsurface mooring was redeployed with an upward-looking 75-kHz ADCP, without temperature or CTD sensors. It was recovered in August 2011 by the R/V *Ocean Researcher 3*.

Results were presented in 2013 at the ONR workshop in Seattle and the ONR review in Chicago.

RESULTS

Near-field

Satellite remote sensing images often capture NLIWs in the Babuyan channel, between the Luzon mainland and Fuga Island. These NLIWs are generated at a 200-m tall sill west of Babuyan channel. We observed one sizeable, ~ 10 -m amplitude, nonlinear internal wave train 10 km east of the sill. Four days of towed CTD measurements were taken during the spring tide near the generation site of internal tides suggested by numerical models. The observed depth integrated energy flux was prevailingly westward at 16 kW m^{-1} for the diurnal internal tide and 18 kW m^{-1} for the semidiurnal internal tide, in

good agreement with model results. Hydraulic jumps were observed between two Philippine islands, Fuga and Dalupiri islands, by the TOWCTD. Vertical overturnings of order 10 m with 50 m horizontal scales were observed.

Far-field

Five large-amplitude internal solitary waves (ISWs) propagating westward on the upper continental slope in the northern South China Sea were observed in May–June 2011 with nearly full-depth measurements of velocity, temperature, salinity, and density (Fig. 2). As they shoaled at least three waves reached the convective breaking limit: along-wave current velocity exceeded the wave propagation speed C (Fig. 3). Vertical overturns of ~ 100 m were observed within the wave cores; estimated turbulent kinetic energy was up to $1.5 \times 10^{-4} \text{ W kg}^{-1}$. In the cores and at the pycnocline, the gradient Richardson number was mostly < 0.25 . The maximum ISW vertical displacement was 173 m, 38% of the water depth. Observed ISWs had greater available potential energy (APE) than kinetic energy (KE) (Fig. 4). For one of the largest observed ISWs the total wave energy per unit meter along the wave crest was 553 MJ m^{-1} , more than three orders of magnitude greater than observed on the Oregon shelf. Pressure work contributed 77% and advection 23% of the energy flux (Fig. 5). The energy flux nearly equaled the CE , where C is the wave propagation speed and E the wave total energy. The Dubriél–Jacotin–Long model with and without a background shear predicts neither the observed $APE > KE$ nor the subsurface maximum of the along-wave velocity for shoaling ISWs, but does simulate the total energy and the wave shape. Including the background shear in the model leads to the formation of a surface trapped core.

A numerical model, the Luzon Strait Ocean Nowcast/Forecast System developed at the U.S. Naval Research Laboratory that covers the northern South China Sea and the Kuroshio, is used to interpret the variation of internal tidal energy observed by an array of three moorings in 2006-2007 on the Dongsha slope. Internal tides are generated primarily at the two submarine ridges in Luzon Strait. At the western ridge generation site, the westward energy flux of the diurnal internal tide is sensitive to the stratification and isopycnal slope associated with the Kuroshio (Fig. 6). The variation of internal tidal energy on the continental slope and Dongsha plateau can be attributed to the variation in tidal beam propagation in the northern South China Sea (Fig. 7).

IMPACT/APPLICATION

Numerical models suggest strong internal tides are generated as barotropic tides interact with two prominent submarine ridges in the Luzon Strait. These internal tides are believed to be the sources of nonlinear internal waves often observed in the South China Sea. The strength of internal tides is modulated by the barotropic tidal forcing, the strength of the Kuroshio current, the background stratification, and the strength of the Kuroshio front. It is important to quantify the barotropic to baroclinic tidal energy conversion, dissipation within the Luzon Strait, the energy fluxes toward the South China Sea and Pacific Ocean, and the ultimate fate of the internal tidal energy.

RELATED PROJECTS

Studying the Origin of the Kuroshio with an Array of ADCP-CTD Moorings (N00014-10-1-0397) as a part of the OKMC DRI: The primary objectives of this observational program are to quantify the origin of the Kuroshio, to quantify its properties at the origin and as it evolves downstream, and to study the effects of mesoscale eddies on Kuroshio transport. Kuroshio transport off Luzon is computed

using direct velocity measurements from a moored array. The annual mean transport is 15 Sv. Large variations of >10 Sv within 10s of days are caused by westward propagating eddies interacting with the Kuroshio.

PUBLICATIONS (wholly or in part supported by this grant)

- Lien, R.-C., F. Henyey, B. Ma, and Y.J. Yang. 2013. Large-amplitude internal solitary waves observed in the northern South China Sea: Properties and energetics, *J. Phys. Oceanogr.*, Early online release, doi: 10.1175/JPO-D-13-088.1. [published, refereed]
- Ma, B., R.-C. Lien, and D. S. Ko, The variability of internal tides in the Northern South China Sea, *J. Oceanogr.*, Early online release, doi: 10.1007/s10872-013-0198-0. [published, refereed]
- Lien, R.-C., E.A. D'Asaro, F. Henyey, M.-H. Chang, T.-Y. Tang, Y.-J. Yang. 2012. Trapped core formation within a shoaling nonlinear internal wave. *J. Phys. Oceanogr.*, **42**, 511–525, doi: 10.1175/2011JPO4578.1. [published, refereed]
- Farmer, D.M., M.H. Alford, R.-C. Lien, Y.J. Yang, M.-H. Chang, and Q. Li. 2011. From Luzon Strait to Dongsha Plateau: Stages in the life of an internal wave. *Oceanography* **24**, 64–77, doi: 10.5670/oceanog.2011.95. [published, refereed]
- Chang, M.-H., R.-C. Lien, Y.-J. Yang, and T.-Y. Tang. 2011. Nonlinear internal wave properties estimated with moored ADCP measurements. *J. Atmos. Ocean. Technol.*, **28**, 802–815, doi: 10.1175/2010JTECHO814.1. [published, refereed]
- Klymak, J.M., M.H. Alford, R. Pinkel, R.-C. Lien, Y.-J. Yang, and T.-Y. Tang. 2011. The breaking and scattering of the internal tide on a continental slope. *J. Phys. Oceanogr.*, **41**, 926–945, doi: 10.1175/2010JPO4500.1. [published, refereed]
- Alford, M.H., R.-C. Lien, H. Simmons, J. Klymak, S. Ramp, Y.-J. Yang, D. Tang, and M.-H. Chang. 2010. Speed and evolution of nonlinear internal waves transiting the South China Sea. *J. Phys. Oceanogr.*, **40**, 1338–1355, doi: 10.1175/2010JPO4388.1. [published, refereed]

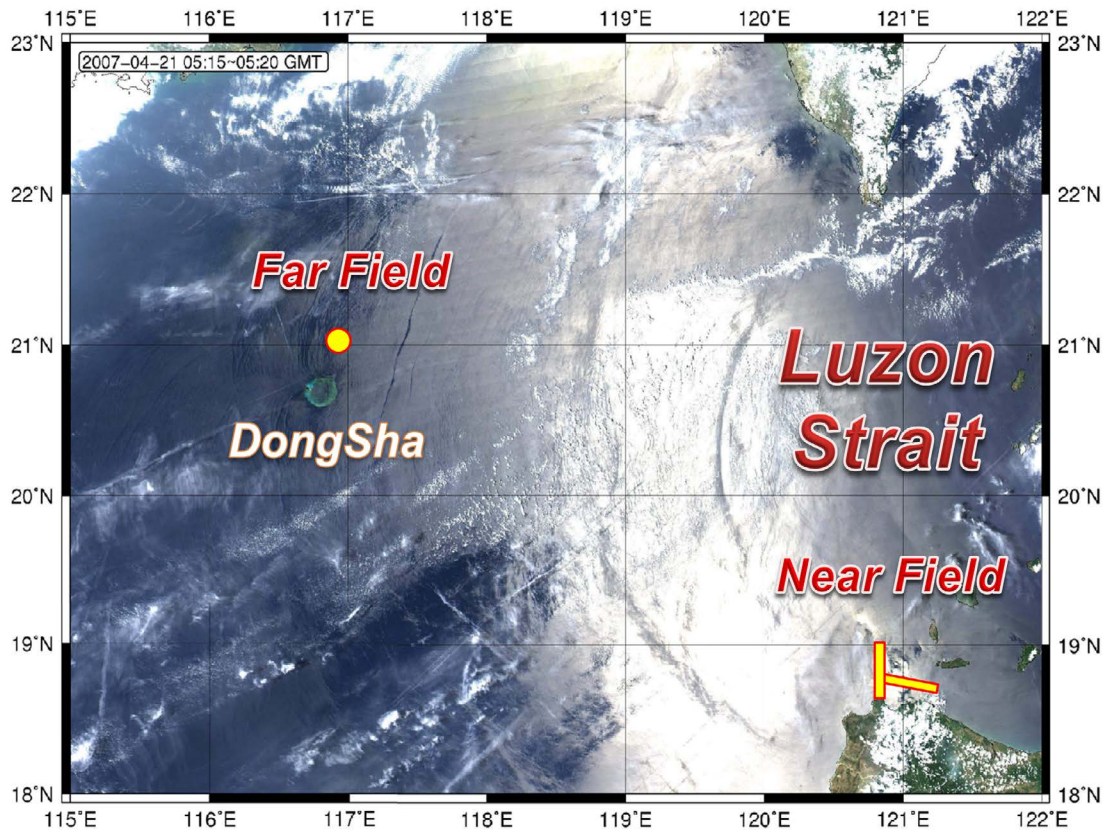


Figure 1. MODIS image taken in 2007 and the general area of near-field and far-field experiments. The near-field was performed using a towed CTD chain (TOWCTD) during July 25 – August 4, 2011 in the southern Luzon Strait (the two yellow boxes). The far-field was performed using a surface mooring and a subsurface mooring (yellow dot) during May 30 – July 3, 2011.

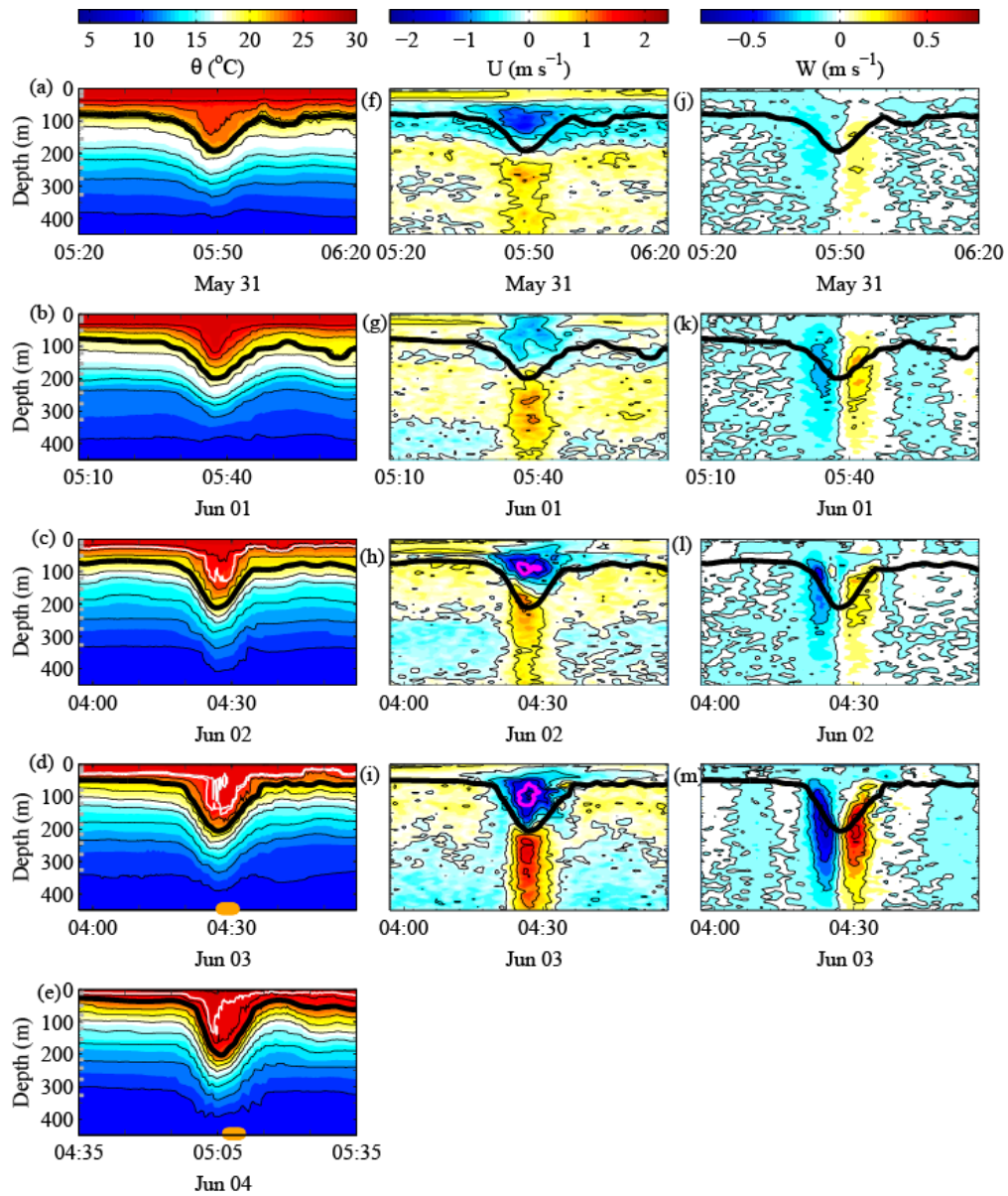


Figure 2. Contour plots of temperature (a–e), along-wave velocity (f–i), and vertical velocity (j–m) of five ISWs observed 31 May–4 June 2011. Thick black curves represent the isopycnal of the maximum vertical displacement. The magenta curves in panels (h) and (i) are contours of the wave propagation velocity. Within the magenta contours, the current velocity is greater than the wave propagation velocity, indicating convective instability. The brown dots in panels (d) and (e) represent near bottom gravitational instability events behind the waves.

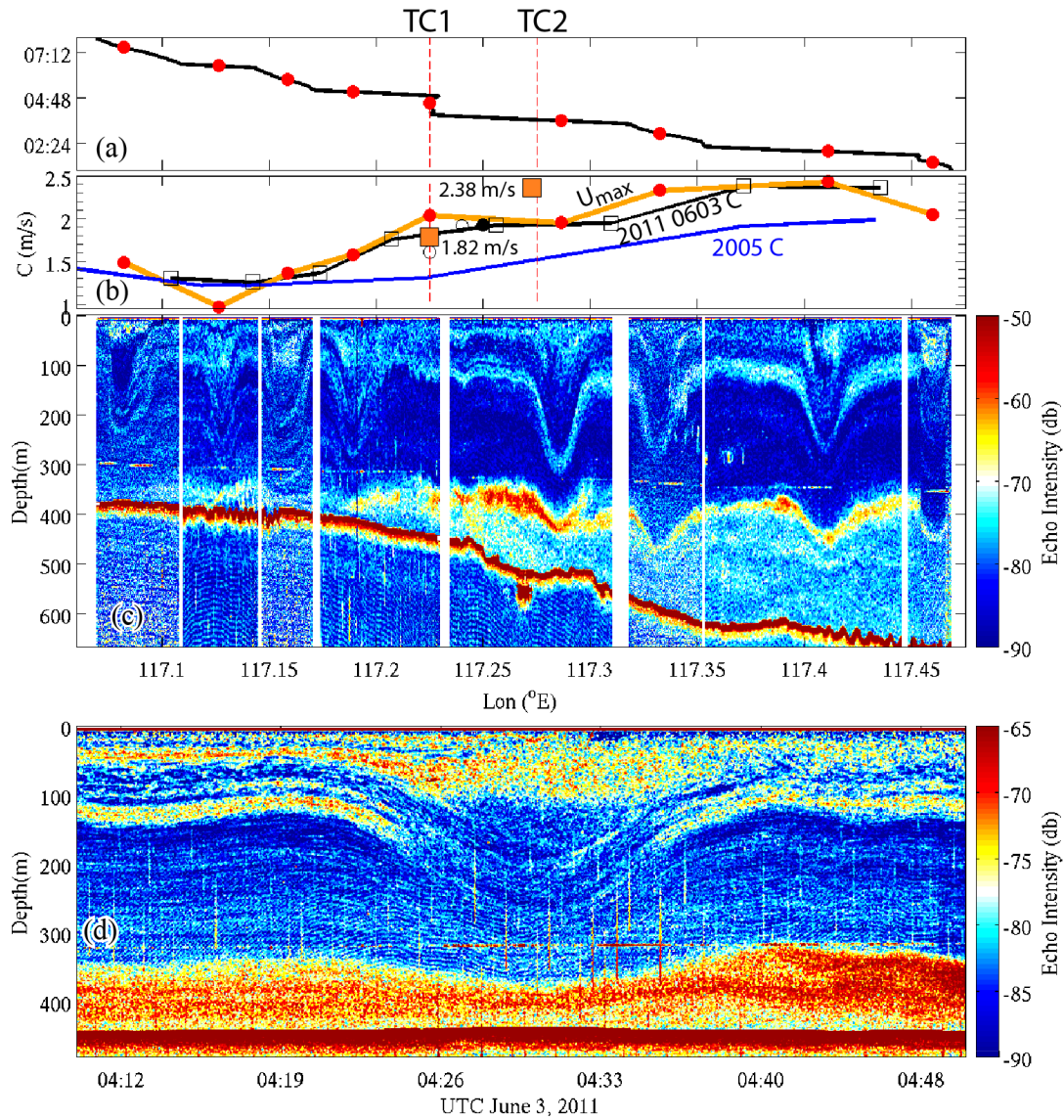


Figure 3. Echo sounder measurements of an ISW taken on 3 June 2011 as the R/V OR3 tracked the wave. Panel (a) shows the ship track as a function of time and longitude. The red dots indicate the time and longitude of the center of the wave. The black curve and black squares in panel (b) show the wave propagation speed computed from the positions and times of the wave center, and the brown curve with the red dots represents the maximum along-wave velocity. The black dot shows the estimate of wave propagation speed computed using the difference of arrival time on the subsurface and surface moorings. Two brown squares show the wave propagation speed computed using the shipboard radar. The blue curve shows the propagation speed of a similar wave observed at the same location in 2005 (Lien et al., *J. Phys. Oceanogr.*, 42, 511-525, 2012). Panel (c) shows the echo sounder images during eight encounters with the wave. Panel (d) shows the echo sounder during the 5th encounter when the ship was maintained on station about 4 km north of the surface mooring. The two vertical lines on panels (a) and (b) mark the positions of the surface mooring (TC1) and the subsurface mooring (TC2).

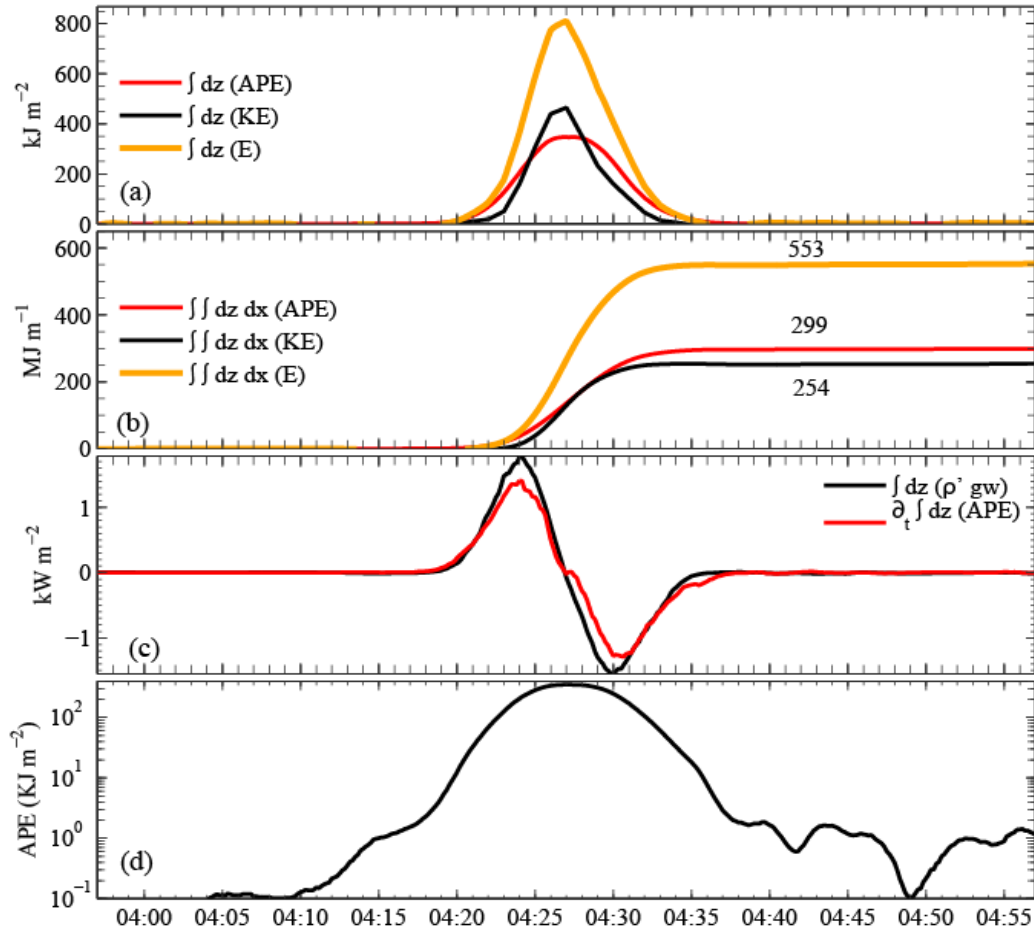


Figure 4. Time variation of ISW energy on 3 June 2011 observed by surface mooring instruments. Time series of (a) the depth integrated APE (red), KE (black), and the total energy E (brown), (b) the along-wave and depth integrated APE (red), KE (black), and E (brown), (c) the time rate change of APE (red) and the depth integrated buoyancy flux (black), and (d) the depth integrated APE plotted in logarithm scale.

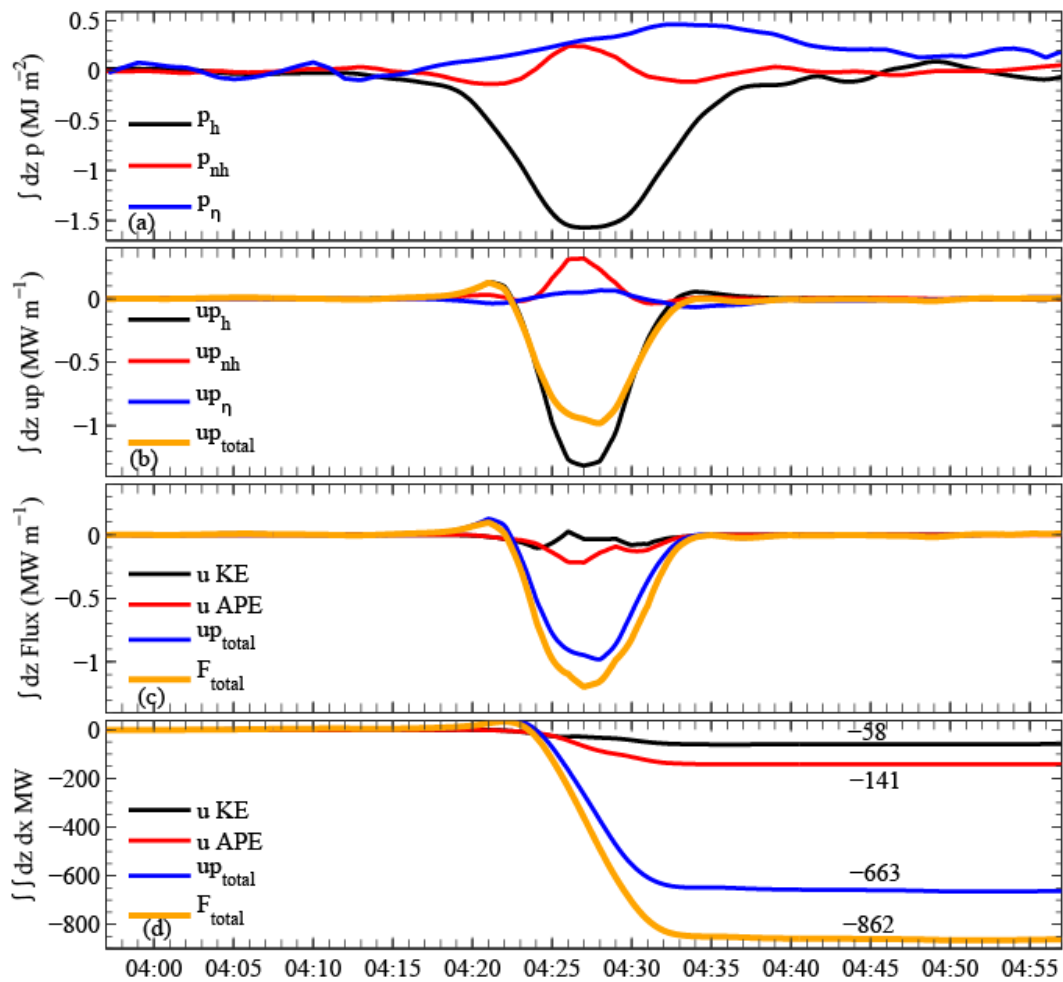


Figure 5. ISW properties from 3 June 2011. Vertically integrated time variations of (a) hydrostatic pressure (black), non-hydrostatic pressure (red), and external pressure due to surface elevation disturbance (blue), (b) velocity-pressure work of hydrostatic pressure (black), non-hydrostatic pressure (red), external pressure due to surface elevation (blue), and the total velocity-pressure work (brown), and (c) horizontal advection of KE (black), horizontal advection of APE (red), the total velocity-pressure work (blue), and the total flux (the sum of the above three components) (brown). Panel (d) shows the along-wave integration of (c).

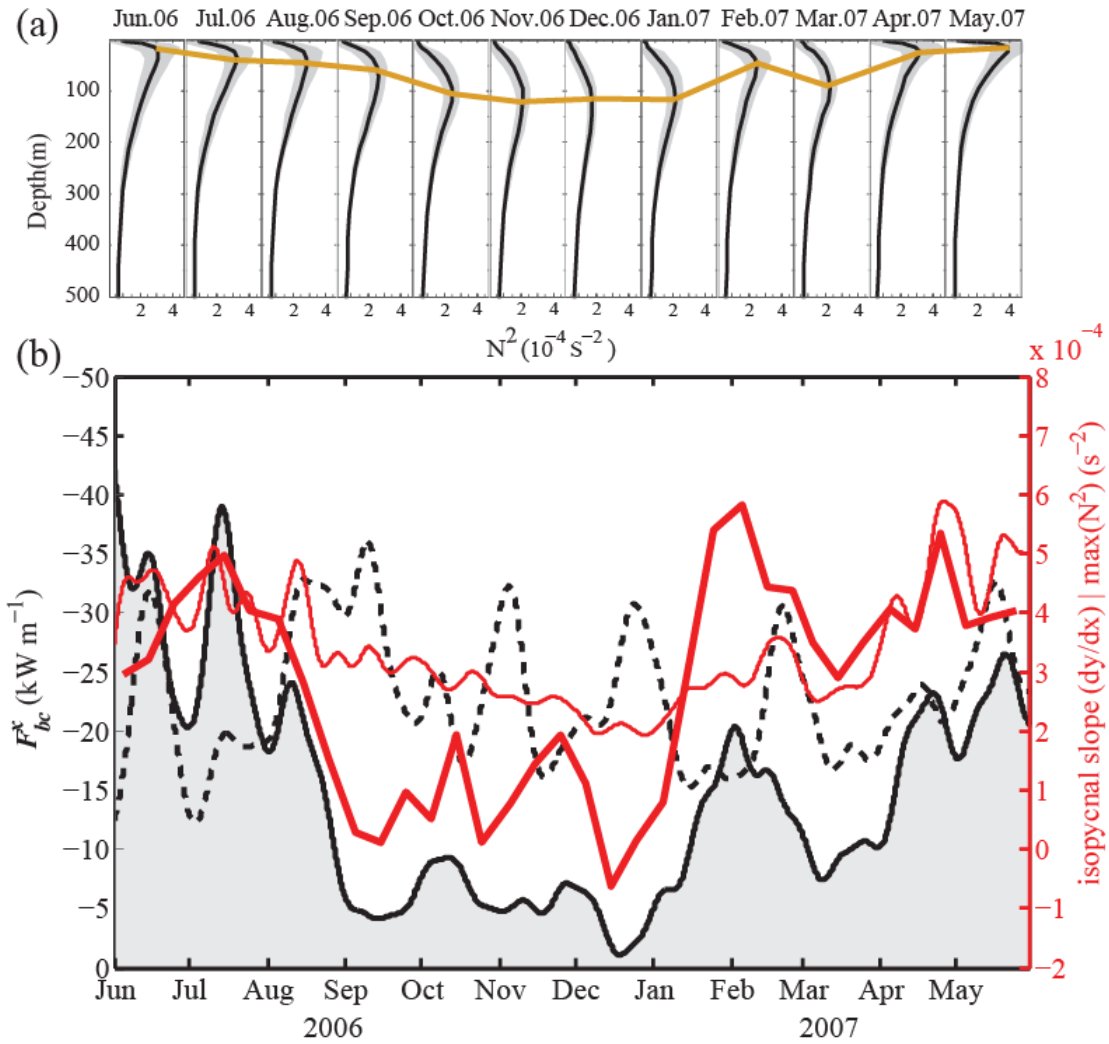


Figure 6 (a) The monthly mean buoyancy profiles and the depth of maximum stratification (brown line). (b) The model zonal energy flux and isopycnal slope at $120.5^\circ E$, $21^\circ N$ near the internal tide generation site. Black solid line is the model diurnal internal tide depth integrated energy flux. Black dash line is the model semidiurnal internal tide depth integrated energy flux. The thick red line is the isopycnal slope between $120^\circ E$ and $121^\circ E$. The thin red line is the maximum buoyancy frequency squared.

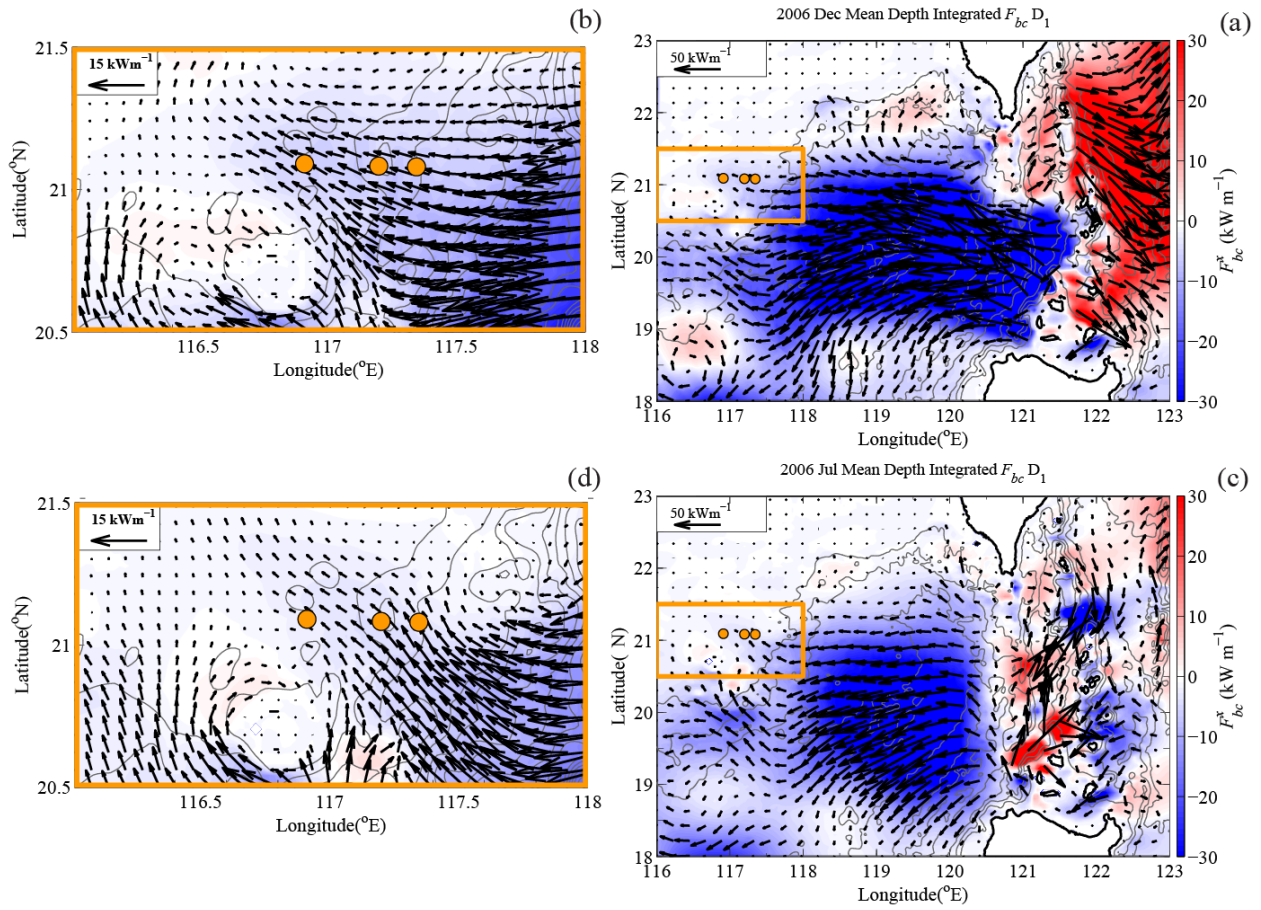


Figure 7. Model results of the depth-integrated diurnal energy flux. The arrows represent the vector of baroclinic diurnal tidal energy flux. The background colors represent its zonal component. (a) December 2006 and (b) detail of the Dongsha plateau, (c) July 2006 and (d) detail of the Dongsha plateau. The red dots indicate the mooring locations. The isobath contour interval is 1000 m for (a) and (c), and 100 m for (b) and (d).